Science & Technology Development Journal 2024, 27(4):3672-3680

Open Access Full Text Article

Research article

Silver Nanoparticles Synthesized from *Phlogacanthus turgidus* Leaf Extract: Catalytic Activity in TMB-H_2O_2 Redox Reactions and their Application in Hydrogen Peroxide Sensing

Dang Van Su[1,*], Phan Thi Thanh Dieu[1], Nguyen Le Kim Thuy[2], Nguyen Thanh Danh[2]

ABSTRACT

Introduction: Among metal nanoparticles (MNPs), silver nanoparticles (AgNPs) have attracted particular attention because of their excellent electrical and optical properties. Notably, colorimetric sensors incorporating metal nanoparticles have garnered significant attention from scientists in biochemical analysis, offering a simple solution. Here, we report the use of AgNPs in a hydrogen peroxide (H_2O_2) sensor. **Methods :** AgNPs were synthesized from *Phlogacanthus turgidus* leaf extract, H_2O_2 was used to oxidize colorless 3,3',5,5'-tetramethylbenzidine (TMB) into blue ox-TMB, and the reaction was catalyzed by $AgNO_3$. Measuring the resulting solution spectrophotometrically helped to determine the concentration of ox-TMB, thereby determining the concentration of H_2O_2 produced. **Results:** The UV–Vis spectrum of the AgNPs synthesized from *Phlogacanthus turgidus* leaf extract exhibited a prominent absorption peak at 427 nm. The linear range was determined to be 100–300 μM. The linear regression equation is $y = 0.91574 + 3.10484 \times 10^{-4}\ C_{H2O2}$, with an SD value of 0.00438. The results revealed that the limit of detection (LOD) of H_2O_2 through the color reaction between TMB and H_2O_2 in AgNP catalysis was 46.55 μM, and the limit of quantification (LOQ) was 141.07 μM. **Conclusion:** On the basis of the results of the optimal conditions for TMB oxidation in the presence of AgNPs, we can evaluate the applicability of this material as a H_2O_2 sensor.

Key words: AgNPs, green synthesis, Phlogacanthus turgidus, H_2O_2 sensor

[1] *Ho Chi Minh City University of Industry and Trade*

[2] *Institute of Chemical Technology, Vietnam Academy of Science and Technology*

Correspondence

Dang Van Su, Ho Chi Minh City University of Industry and Trade

Email: sudv@huit.edu.vn

History

- Received: 2024-07-30
- Revised: 2024-12-11
- Accepted: 2024-12-27
- Published Online: 2024-12-31

DOI :

https://doi.org/10.32508/stdj.v27i4.4341

INTRODUCTION

MNPs have recently become a topic of interest because of their diverse applications [1–6]. MNPs are important materials used in the fields of biomedicine, optics, the environment, catalysis and electrochemistry, such as biosensors [7–11]. Among MNPs, AgNPs have received particular attention because of their excellent electrical and optical properties [12]. H_2O_2 is a powerful oxidizing agent with various applications in medicine and industry. It is commonly known as a bleaching and disinfecting agent. However, proper handling is crucial to ensure safety and effectiveness, as it is highly corrosive and can alter stem cells and pose acute and chronic toxicity risks to aquatic environments [13–15]. H_2O_2 is measured and quantified across a wide range of sample matrices, including environmental samples (water and soil), human fluids (sweat and blood), and cell and tissue cultures. Various methods are employed for this purpose, including optical techniques (colorimetry, chemiluminescence, and fluorescence), as well as electrochemical methods (potentiometry, voltammetry, and amperometry). Notably, colorimetric sensors incorporating metal nanoparticles have garnered significant attention from scientists in biochemical analysis, offering a simple solution [16].

Recently, many studies have investigated the green synthesis and application of AgNPs in H_2O_2 sensors. Nurul Ismillayli et al. (2024) reported the use of microwave-assisted synthesis of AgNPs as a colorimetric sensor for H_2O_2 [17]. Ramesh Vinayagam et al. (2024) studied the structural characterization of marine macroalgae-derived AgNPs and their colorimetric sensing of H_2O_2 [18]. Haodong Shen et al. (2023) reported a one-step synthesis of nanosilver embedding laser-induced graphene for H_2O_2 sensors [19]. However, there has been no research on the synthesis of AgNPs from *Phlogacanthus turgidus* leaf extract for application as H_2O_2 detectors on the basis of the reduction reactions of TMB and H_2O_2 in AgNP catalysis. The reduction in TMB is illustrated in Scheme 1. In this strategy, the AgNPs act as catalysts, and the oxidation product of TMB possesses a blue color, which can be determined via UV–Vis spectroscopy. The catalytic mechanism of AgNPs involves three primary steps: (1) the generation of hydroxyl radicals (OH·),

Cite this article : Su D V, Dieu P T T, Thuy N L K, Danh N T. **Silver Nanoparticles Synthesized from *Phlogacanthus turgidus* Leaf Extract: Catalytic Activity in TMB-H_2O_2 Redox Reactions and their Application in Hydrogen Peroxide Sensing**. *Sci. Tech. Dev. J.* 2024; 27(4):3672-3680.

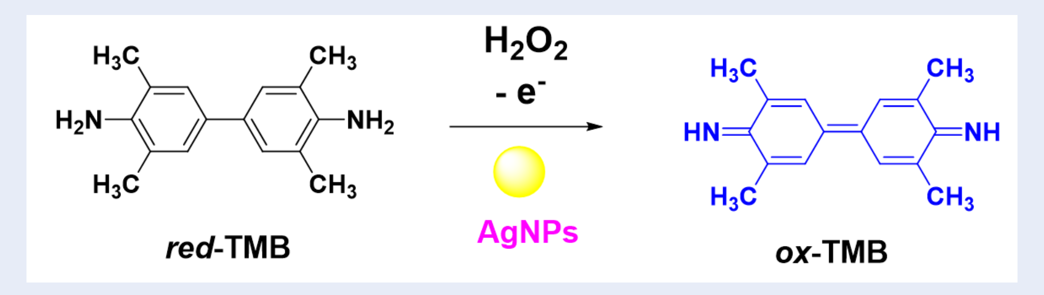

Scheme 1: Oxidation mechanism of TMB using H_2O_2 in the presence of a AgNP catalyst.

(2) the production of oxygen (O_2), and (3) electron transfer, as illustrated in Scheme 1[20]. Moreover, the extract of the *Phlogacanthus turgidus* leaf contains high levels of polyphenols[21], which have the ability to reduce and stabilize metallic nanoparticles. In this study, *Phlogacanthus turgidus* leaf extract was used to synthesize AgNPs, and the catalytic ability of AgNPs in the redox reaction between H_2O_2 and TMB was investigated.

MATERIALS AND METHODS

Materials

Phlogacanthus turgidus leaves were collected from Bu Gia Map National Park, Binh Phuoc Province, Vietnam. Chemicals including silver nitrate ($AgNO_3$), 3,3',5,5'-tetramethylbenzidine ($C_{16}H_{20}N_2$), hydrogen peroxide (H_2O_2), acetic acid (CH_3COOH) and sodium acetate (CH_3COONa), which were of analytical grade without further purification, were purchased from Acros Co., Belgium. Deionized water was thoroughly utilized in all the experiments.

Methods

Synthesis of AgNPs from Phlogacanthus turgidus leaf extract

The synthesis of silver nanoparticles (AgNPs) was performed via *Phlogacanthus turgidus* leaf extract, following previous reports[2,5]. Specifically, 0.25 mL of *Phlogacanthus turgidus* leaf extract was mixed with 5 mL of an aqueous $AgNO_3$ solution under reaction conditions of 2.0 mM silver ion concentration, 80°C, and a reaction time of 70 minutes. The formation of AgNPs was verified via UV–Vis spectrophotometry. The synthesized AgNP solution was subsequently stored at 8°C for future applications.

Determination of the optimal temperature for the TMB and H_2O_2 reactions with the AgNP catalyst

To optimize the reaction temperature, 400 μL of 5 mM TMB, 2 mL of acetate buffer solution (pH 5), 600 μL of 400 μM H_2O_2, and 150 μL of the synthesized AgNP solution were each carefully added to a 10 mL bottle. The bottle was covered with foil to protect it from light and placed in a thermostatic bath at various temperatures (30°C, 35°C, 40°C, 45°C, 50°C, 55°C, and 60°C) for 30 minutes. Following incubation, UV–Vis spectroscopy was used to measure the absorbance of the solutions to determine the optimal temperature for the reaction of TMB and H_2O_2 in the presence of the AgNP catalyst.

Determination of the optimal time for the TMB and H_2O_2 reactions with the AgNP catalyst

To determine the optimal reaction time, 400 μL of 5 mM TMB, 2 mL of acetate buffer solution (pH 5), 600 μL of 400 μM H_2O_2, and 150 μL of the AgNP solution were added to a 10 mL container, which was carefully covered with foil. This container was then placed in a thermostatic reaction tank set to the optimal temperature. UV–Vis spectroscopy measurements were taken at 10-minute intervals to identify the optimal reaction time for the interaction between TMB and H_2O_2 in the presence of the AgNP catalyst.

Determination of the optimal pH for the TMB and H_2O_2 reactions with the AgNP catalyst

To optimize the pH for the reaction, 400 μL of 5 mM TMB, 2 mL of acetate buffer solution at various pH values, 600 μL of 400 μM H_2O_2, and 150 μL of the AgNP solution were added to 10 mL bottles and covered with foil. These bottles were then placed in a thermostatic bath set to the optimal temperature and time. UV−Vis spectroscopy measurements were conducted to identify the optimal pH for the TMB and H_2O_2 reactions in the presence of the AgNP catalyst.

Determination of the optimal AgNP concentration for the TMB and H_2O_2 reactions with the AgNP catalyst

To optimize the concentration of AgNPs, 400 μL of 5 mM TMB, 2 mL of acetate buffer solution (adjusted to the optimal pH), 600 μL of 400 μM H_2O_2, and varying volumes of the AgNP solution (60 μL, 70 μL, 80 μL, 90 μL, 100 μL, 110 μL, 120 μL, and 130 μL) were added to separate 10 mL bottles, each covered with foil. These bottles were then placed in a thermostatic bath set to the optimal temperature and time. UV−Vis spectroscopy was used to determine the optimal concentration of AgNPs for the TMB and H_2O_2 reactions.

Determination of the optimal TMB concentration for TMB and H_2O_2 reactions with AgNP catalysts

To determine the optimal concentration of TMB, 2 mL of acetate buffer solution (adjusted to the optimal pH), 600 μL of 400 μM H_2O_2, the optimal volume of AgNP solution (determined *in section 2.5*), and varying concentrations of TMB (400 μL of 3 mM, 3.5 mM, 4 mM, 4.5 mM, 5 mM, 5.5 mM, 6 mM, or 6.5 mM) were added to separate 10 mL bottles, which were covered with foil. These bottles were then placed in a thermostatic bath set to the optimal temperature and time. UV−Vis spectroscopy was performed to determine the optimal TMB concentration for the TMB and H_2O_2 reactions catalyzed by the AgNPs.

Determination of the linear range and limit of detection (LOD) value

To determine the optimal concentration of H_2O_2, 400 μL of TMB, 2 mL of acetate buffer solution (adjusted to the optimal pH), and the optimal volume of AgNP solution were combined with varying concentrations of H_2O_2 (600 μL of 10 μM, 50 μM, 100 μM, 150 μM, 200 μM, 250 μM, 300 μM, 350 μM, and 400 μM) in separate 10 mL bottles, each covered with foil. These bottles were placed in a thermostatic bath set to the optimal temperature and time. UV−Vis spectroscopy was conducted on the solutions to identify the optimal concentration of H_2O_2 for the reaction with TMB catalyzed by AgNPs. The limits of detection (LODs) and limits of values were calculated via Equations (1) and (2), respectively:

$$\begin{aligned} LOD &= 3.3 \times \frac{SD}{a} \\ &= 3.3 \times \frac{0.0438}{3.10484 \times 10^{-4}} = 46.55\ \mu M \end{aligned} \tag{1}$$

$$\begin{aligned} LOQ &= 10 \times \frac{SD}{a} \\ &= 10 \times \frac{0.0438}{3.10484 \times 10^{-4}} = 141.07\ \mu M \end{aligned} \tag{2}$$

where SD and a are the standard deviation and slope of the linear regression line, respectively.

RESULTS AND DISCUSSION

Synthesis of AgNPs from *Phlogacanthus turgidus* leaf extract

Figure 1a shows that the peak absorption of the AgNPs synthesized from *Phlogacanthus turgidus* leaf extract was in the wavelength range of 400–500 nm. The UV−Vis spectrum of the AgNPs synthesized from *Phlogacanthus turgidus* leaf extract exhibited a surface plasmon resonance (SPR) peak at 427 nm. Microscopy images (Figure 1b and Figure 1c) revealed that the structure of the AgNPs consisted mostly of spheres with an average size of 13 nm, which aligns with the findings of a previous study[2].

Optimization of the TMB and H_2O_2 reactions with the AgNP catalyst

Figure 2 shows the UV−Vis spectra of TMB oxidation as a function of reaction temperature. The absorption spectra were recorded over a temperature range from 20°C to 60°C. The data indicated that the absorbance at a wavelength of 654 nm increased progressively with temperature, reaching a maximum at 35°C. Beyond this temperature, a decrease in absorbance was observed, which was likely attributed to the thermal instability of ox-TMB at higher temperatures. Accordingly, 35°C was identified as the most favorable temperature for the efficient oxidation of TMB by H_2O_2, facilitated by the AgNP catalyst.

Results of the optimal time for the reaction of TMB and H_2O_2 with the AgNP catalyst

The effect of reaction time on TMB oxidation was evaluated at the optimal temperature of 35°C, with measurements taken at 10-minute intervals to identify the optimal reaction duration. The absorbance data obtained via UV−Vis spectroscopy are presented in Figure 3. Superimposing the absorption spectra for various time points revealed that the reaction

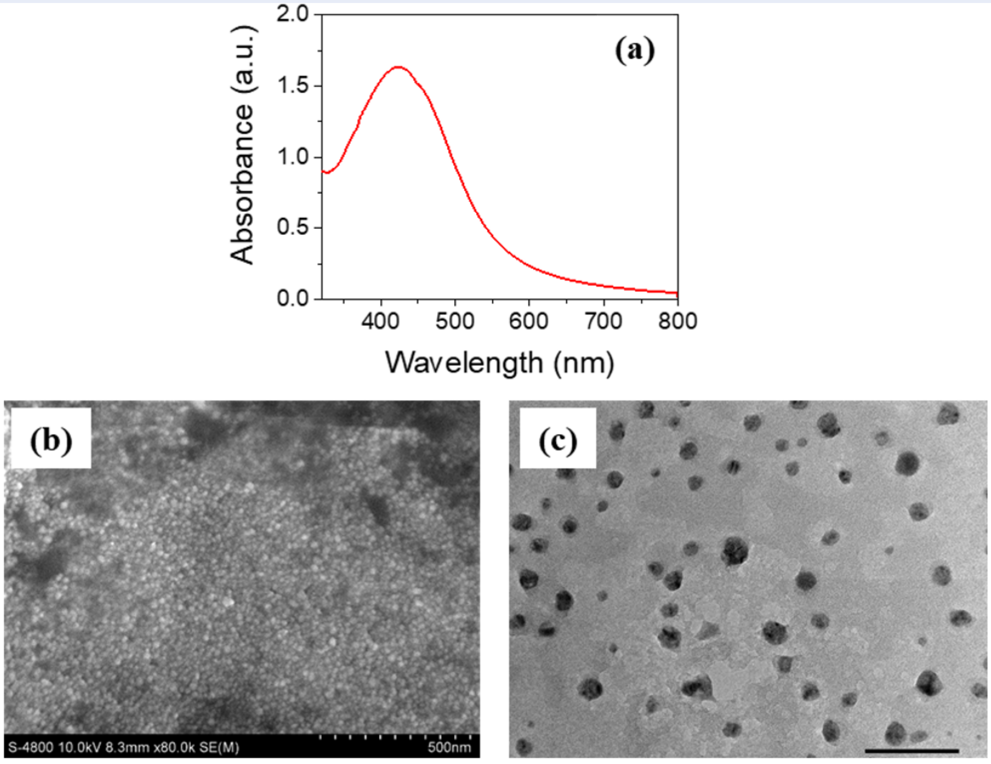

Figure 1: UV–Vis spectra (a) and SEM (b) and TEM (c) images of AgNPs synthesized from *Phlogacanthus turgidus* leaf extract

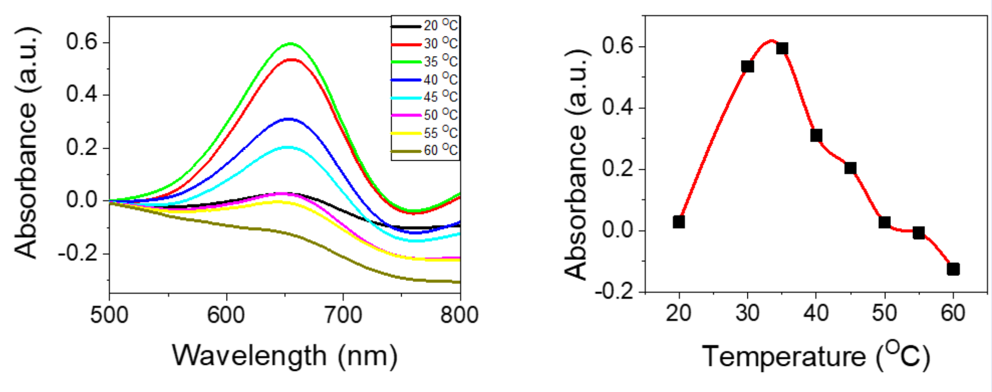

(a) (b)

Figure 2: Absorption spectra from the temperature investigation with the AgNP catalyst (a) and the dependence of the absorbance on the reaction temperature (with the AgNP catalyst) (b).

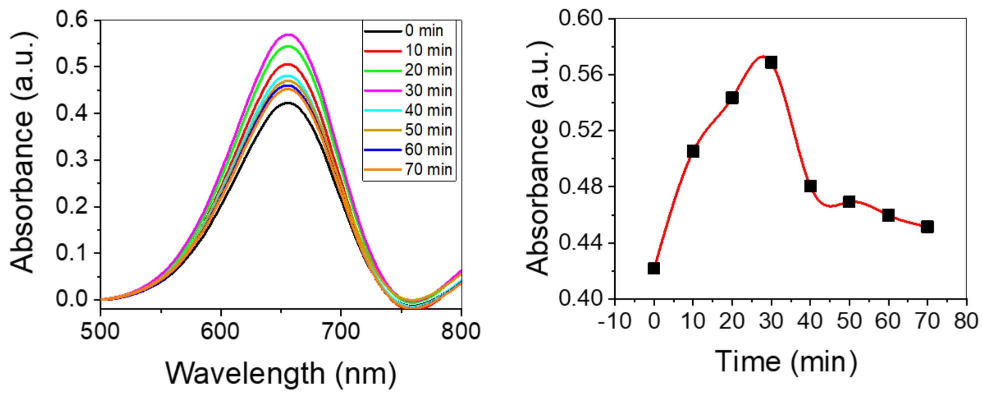

(a) (b)

Figure 3: Absorption spectra over time (a) and dependence of the absorbance on the reaction time with the AgNP catalyst (b).

conducted for 30 minutes presented the highest absorbance intensity at 654 nm. This observation suggests that extended reaction times under these conditions may lead to the degradation of *ox*-TMB. Therefore, a reaction time of 30 min was determined to be the most suitable condition for the oxidation of TMB by H_2O_2 in the presence of the AgNP catalyst, starting from the moment the sample was introduced into the thermostatic bath.

Results of the optimal pH for the reaction of TMB and H_2O_2 with the AgNP catalyst

pH plays a principal role in regulating the oxidation rate of TMB. UV–Vis spectra were recorded and compared for samples prepared under various pH conditions, as illustrated in Figure 4. The data revealed that samples with a pH of 4 presented the highest absorbance intensity at 654 nm, while this intensity progressively decreased for samples with low or high pH values. This trend can be attributed to the reaction equilibrium under highly acidic conditions ($pH < 4.0$) shifting toward the formation of *red*-TMB. Conversely, at higher pH values, the decreasing formation efficiency of the colored product at 654 nm may result from the elevated redox potential of the substrates, leading to decreased susceptibility to oxidation[22]. Consequently, pH 4 was identified as the optimal condition and was selected for further exploration of the factors influencing the TMB redox process with H_2O_2 in the presence of an AgNP catalyst.

The effects of the optimal AgNP concentration on the TMB and H_2O_2 reactions

A survey was conducted to investigate the influence of the AgNP catalyst volume on the absorption intensity of the samples in solution. The absorption spectra of the solutions containing TMB, acetate buffer (pH 4), H_2O_2, and various volumes of the AgNP catalyst were analyzed (Figure 5). At a wavelength of 654 nm, the absorption intensity increased progressively as the AgNP volume increased from 60 μL to 120 μL under constant conditions of TMB concentration, acetate buffer, and H_2O_2. However, a significant decrease in the absorption intensity was observed in the sample containing 130 μL of the AgNP catalyst. This indicated that increasing the catalyst volume increased the surface area, thereby improving the catalytic efficiency of the oxidation–reduction reaction. Nevertheless, an excessive amount of AgNPs likely resulted in the decomposition of H_2O_2, reducing the reaction yield. Therefore, 120 μL of AgNP catalyst was identified as the optimal volume and was selected for subsequent investigations of other reaction parameters.

The effects of the optimal TMB concentration on the TMB and H_2O_2 reactions with the AgNP catalyst

The TMB concentration is a critical parameter for evaluating the reaction efficiency between TMB and H_2O_2 in the presence of the synthesized AgNP catalyst. Figure 6 shows the dependence of the reaction efficiency on the TMB concentration through changes in the absorption intensity observed in the

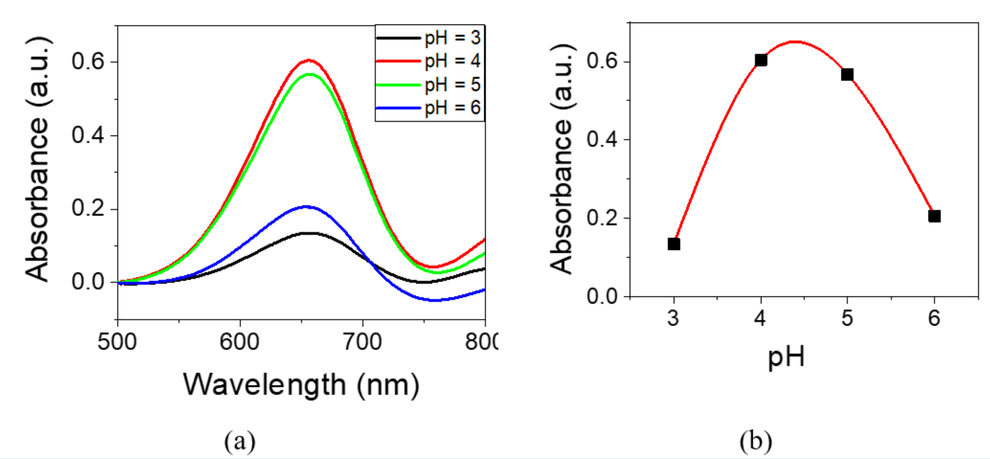

Figure 4: Absorption spectrum of the pH survey (a) and dependence of the absorbance on the pH value of the AgNP catalyst (b).

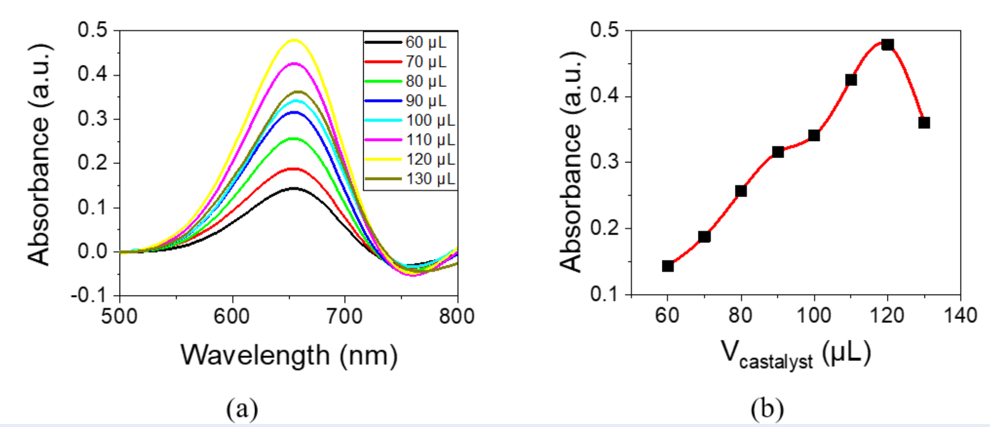

Figure 5: Absorption spectrum of the AgNP catalyst quantity survey (a), and the absorption depends on the amount of AgNP catalyst (b).

UV–Vis spectra at 654 nm. The results revealed that the absorption intensity increased with increasing TMB concentration, reaching a maximum at 5.5 mM. Above this concentration, the absorbance decreased significantly, likely due to the oxidation of monoamine groups in TMB at higher concentrations. Consequently, a TMB concentration of 5.5 mM was selected as the optimal condition for the redox reaction between TMB and H_2O_2 in the presence of the AgNP catalyst.

Influence of the H_2O_2 concentration on the TMB and H_2O_2 reactions with the AgNP catalyst

Figure 7 shows the dependence of the absorbance values on the H_2O_2 concentration. The absorbance intensity at 654 nm increased with increasing H_2O_2 concentration, reaching a maximum at 350 μM. Beyond this concentration, the TMB concentration appeared insufficient to react fully with H_2O_2. A linear relationship was observed within the range of 100–300 μM, described by the regression equation y = 0.91574 + 3.10484×10^{-4} C_{H2O2}, with a standard deviation (SD) of 0.00438. The limit of detection (LOD) for H_2O_2, which is based on the colorimetric reaction between oxidized TMB (ox-TMB) and H_2O_2

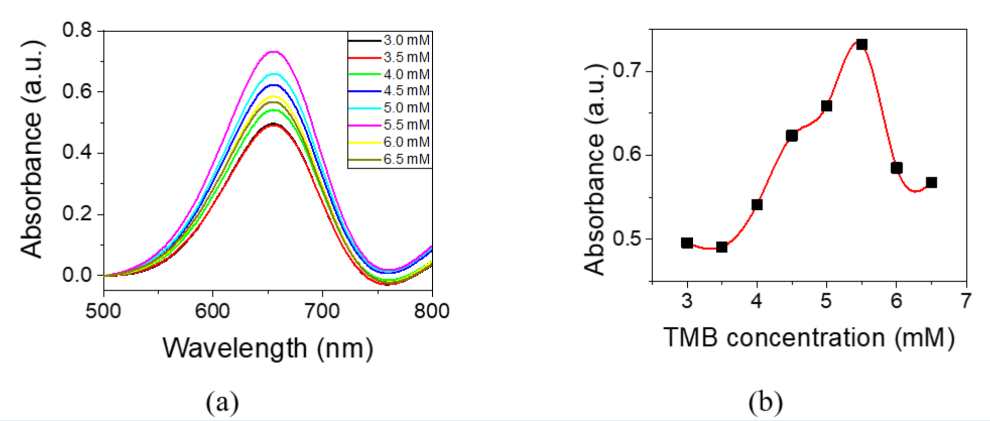

Figure 6: Absorption spectrum of the TMB concentration survey (a) and dependence of the absorbance on the TMB concentration with the AgNP catalyst (b).

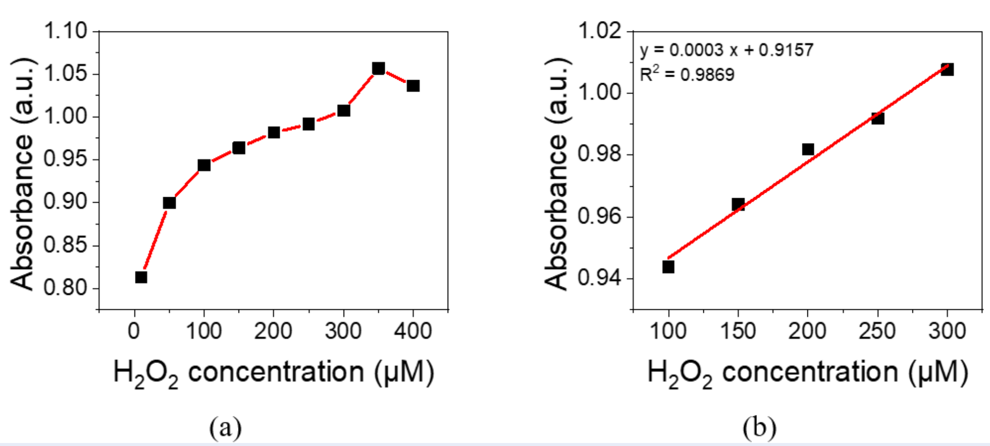

Figure 7: Absorbance dependence on the H2O2 concentration.

catalyzed by AgNPs, was determined to be 46.55 μM, with a limit of quantification (LOQ) of 141.07 μM. These findings, combined with the optimal conditions for TMB oxidation shown in Table 1, underscore the potential of AgNPs as effective catalysts in the TMB-H_2O_2 redox reaction, demonstrating their applicability as sensitive H_2O_2 sensors.

CONCLUSIONS

AgNPs were synthesized from *Phlogacanthus turgidus* leaf extract, resulting in absorption peaks in the wavelength range of 400–500 nm. This investigation of the conditions affecting the oxidation of TMB with H_2O_2 with the AgNP catalyst provides the best conditions for the detection of H_2O_2 through the TMB reaction with the AgNP catalyst. The optimal conditions (temperature, time, pH, AgNP concentration, TMB concentration, and H_2O_2 concentration) for TMB oxidation in the presence of H_2O_2 were 35°C, 30 min, pH 4, 120 μL of AgNPs, 5.5 mM TMB, and H_2O_2 concentrations ranging from 100–300 μM. Therefore, we can evaluate the applicability of H_2O_2 in wastewater.

ABBREVIATIONS

None.

ACKNOWLEDGMENTS

None.

AUTHOR’S CONTRIBUTIONS

All authors equally contributed to this work, read and approved the final version of the manscript for publishing.

Table 1: Optimal conditions for TMB oxidation in the presence of AgNPs.

Parameters	Optimal values
Temperature (^{o}C)	35
Time (minute)	30
pH	4.0
AgNPs catalyst (μL)	120
TMB (mM)	5.5
Concentration range linear H2O2 (μM)	100 - 300

FUNDING

This research is funded by the Vietnam National Foundation for Science and Technology Development (NAFOSTED) under grant number 104.99–2021.56

AVAILABILITY OF DATA AND MATERIALS

Data and materials used and/or analyzed during the current study are available from the corresponding author on reasonable request.

ETHICS APPROVAL AND CONSENT TO PARTICIPATE

Not applicable.

CONSENT FOR PUBLICATION

Not applicable.

COMPETING INTERESTS

The authors declare that they have no competing interests.

REFERENCES

1. Ân TNM. Tổng hợp xanh Nano bạc từ AgNO3 và dịch chiết lá diếp cá. Tp. 2016;32:188–92;.
2. Dang VS, Tran HH, Dieu PTT, Tran MT, Dang CH, Mai DT, et al. Effective catalysis and antibacterial activity of silver and gold nanoparticles biosynthesized by Phlogacanthus turgidus. Res Chem Intermed [Internet]. 2022;48(5):2047–67;Available from: https://doi.org/10.1007/s11164-022-04687-9.
3. Ruddaraju LK, Pallela PNVK, Pammi SVN, Padavala VS, Kolapalli VRM. Synergetic antibacterial and anticarcinogenic effects of Annona squamosa leaf extract mediated silver nano particles. Mater Sci Semicond Process [Internet]. 2019;100(April):301–9;Available from: https://doi.org/10.1016/j.mssp.2019.05.007.
4. Saad PG, Castelino RD, Ravi V, Al-Amri IS, Khan SA. Green synthesis of silver nanoparticles using Omani pomegranate peel extract and two polyphenolic natural products: characterization and comparison of their antioxidant, antibacterial, and cytotoxic activities. Beni-Suef Univ J Basic Appl Sci. 2021;10(1);.
5. Nguyen TTN, Vo TT, Nguyen BNH, Nguyen DT, Dang VS, Dang CH, et al. Silver and gold nanoparticles biosynthesized by aqueous extract of burdock root, Arctium lappa as antimicrobial agent and catalyst for degradation of pollutants. Environ Sci Pollut Res. 2018;25(34):34247–61;.
6. Vo TT, Nguyen TTN, Huynh TTT, Vo TTT, Nguyen TTN, Nguyen DT, et al. Biosynthesis of silver and gold nanoparticles using aqueous extract from crinum latifolium leaf and their applications forward antibacterial effect and wastewater treatment. J Nanomater. 2019;2019:1–14;.
7. Bandi R, Alle M, Park CW, Han SY, Kwon GJ, Kim JC, et al. Rapid synchronous synthesis of Ag nanoparticles and Ag nanoparticles/holocellulose nanofibrils: Hg(II) detection and dye discoloration. Carbohydr Polym [Internet]. 2020;240(March):116356;Available from: https://doi.org/10.1016/j.carbpol.2020.116356.
8. Shipway AN, Katz E, Willner I. Nanoparticle arrays on surfaces for electronic, optical, and sensor applications. Angew Chemie (International Ed English). 2000;39(15 SUPPL.):19–52;.
9. Tracey CT, Torlopov MA, Martakov IS, Vdovichenko EA, Zhukov M, Krivoshapkin P V., et al. Hybrid cellulose nanocrystal/magnetite glucose biosensors. Carbohydr Polym [Internet]. 2020;247(February):116704;Available from: https://doi.org/10.1016/j.carbpol.2020.116704.
10. Mohammed FS, Cole SR, Kitchens CL. Synthesis and enhanced colloidal stability of cationic gold nanoparticles using polyethyleneimine and carbon dioxide. ACS Sustain Chem Eng. 2013;1(7):826–32;.
11. Wang F, Ding X, Niu X, Liu X, Wang W, Zhang J. Green preparation of core-shell Cu@Pd nanoparticles with chitosan for glucose detection. Carbohydr Polym [Internet]. 2020;247(February):116647;Available from: https://doi.org/10.1016/j.carbpol.2020.116647.
12. Bonigala B, Kasukurthi B, Konduri VV, Mangamuri UK, Gorrepati R, Poda S. Green synthesis of silver and gold nanoparticles using Stemona tuberosa Lour and screening for their catalytic activity in the degradation of toxic chemicals. Environ Sci Pollut Res. 2018;25(32):32540–8;.
13. Phụ lục 17 - Kèm thông tư số 28/2010/TT-BCT ngày 28 tháng 6 năm 2010 của Bộ Công Thương. Bộ Công Thương. 2014;17:1–7;.
14. Eldridge D, Holstege CP. Hydrogen peroxide. Chemwatch. 2016;(7.1.1.1):1–13;.
15. Chen S, Yuan R, Chai Y, Hu F. Electrochemical sensing of hydrogen peroxide using metal nanoparticles: A review. Microchim Acta. 2013;180(1–2):15–32;.
16. Đồng Huy Giới, Bùi Thị Thu Hương, Phí Thị Cẩm Miện Nguyễn Thị Thúy Hạnh ĐĐN. Tạo cảm biến từ Nano vàng và ADN chức năng để phát hiện nhanh ion thủy ngân trong nước. Tạp chí Khoa học nông nghiệp Việt Nam. 2016;14(3):491–500;.
17. Ismillayli N, Suprapto S, Santoso E, Nugraha RE, Holilah H, Bahruji H, et al. Microwave-assisted synthesis of silver nanoparticles as a colorimetric sensor for hydrogen peroxide. RSC Adv. 2024;14(10):6815–22;.
18. Vinayagam R, Nagendran V, Goveas LC, Narasimhan MK, Varadavenkatesan T, Chandrasekar N, et al. Structural characterization of marine macroalgae derived silver nanoparticles and their colorimetric sensing of hydrogen peroxide. Mater Chem Phys [Internet]. 2024;313(December 2023):128787;Available from: https://doi.org/10.1016/j.matchemphys.2023.128787.

19. Shen H, Liu J, Pan P, Yang X, Yang Z, Li P, et al. One-step synthesis of nanosilver embedding laser-induced graphene for H2O2 sensor. Synth Met [Internet]. 2023;293(December 2022):117235;Available from: https://doi.org/10.1016/j.synthmet.2022.117235.
20. An C zheng; WKTY and X. Intrinsic peroxidase-like activity and the catalytic mechanism of gold @ carbon dots nanocomposites. RSC Adv. 2013;00(1–3):1–8;.
21. Minh PN, Phát NT, Chí MT, Hiển ĐC, Trị MĐ. Thành phần hóa học của toàn cây Thường sơn tía PHLOGACANTHUS TURGIDUS (FUA EX HOOK . F .) LINDAU. 2021;5(3):1341–9;.
22. He W, Liu Y, Yuan J, Yin JJ, Wu X, Hu X, et al. Au@Pt nanostructures as oxidase and peroxidase mimetics for use in immunoassays. Biomaterials [Internet]. 2011;32(4):1139–47;Available from: http://dx.doi.org/10.1016/j.biomaterials.2010.09.040.